Acta Crystallographica Section F
Structural Biology and Crystallization Communications
ISSN 1744-3091

Engineering an improved crystal contact across a solvent-mediated interface of human fibroblast growth factor 1

Akshaya K. Meher,[a,b] Sachiko I. Blaber,[a] Jihun Lee,[a] Ejiro Honjo,[c] Ryota Kuroki[c] and Michael Blaber[a]*

[a]Department of Biomedical Sciences, Florida State University, Tallahassee, FL 32306-4300, USA, [b]Cardiovascular Research Center, University of Virginia, Charlottesville, VA 22908, USA, and [c]Molecular Structural Biology Group, Quantum Beam Sciences Directorate, Japan Atomic Energy Agency, Tokai, Ibaraki 319-1195, Japan

Correspondence e-mail: michael.blaber@med.fsu.edu

Received 31 July 2009
Accepted 12 September 2009

PDB References: human fibroblast growth factor 1, E81A/K101A mutant, 3cqa, r3cqasf; G81A/E82N/K101A mutant, 3crg, r3crgsf; E81S/K101A mutant, 3crh, r3crhgsf; E81S/E82N/K101A mutant, 3cri, r3crisf.

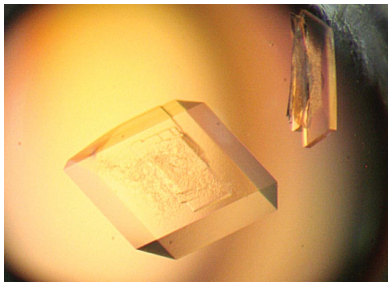

Large-volume protein crystals are a prerequisite for neutron diffraction studies and their production represents a bottleneck in obtaining neutron structures. Many protein crystals that permit the collection of high-resolution X-ray diffraction data are inappropriate for neutron diffraction owing to a plate-type morphology that limits the crystal volume. Human fibroblast growth factor 1 crystallizes in a plate morphology that yields atomic resolution X-ray diffraction data but has insufficient volume for neutron diffraction. The thin physical dimension has been identified as corresponding to the *b* cell edge and the X-ray structure identified a solvent-mediated crystal contact adjacent to position Glu81 that was hypothesized to limit efficient crystal growth in this dimension. In this report, a series of mutations at this crystal contact designed to both reduce side-chain entropy and replace the solvent-mediated interface with direct side-chain contacts are reported. The results suggest that improved crystal growth is achieved upon the introduction of direct crystal contacts, while little improvement is observed with side-chain entropy-reducing mutations alone.

1. Introduction

Neutron diffraction is an important area of interest in structural biology as it provides information on hydrogen and hydrogen bonding, which is one of the most important noncovalent intermolecular forces in biomolecular complexes (Blakeley *et al.*, 2006; Tuan *et al.*, 2007; Niimura & Bau, 2008; Adachi *et al.*, 2009). Neutron diffraction requires crystals of large physical volume (typically 2–10 mm^3) and only a small subset of proteins that crystallize produce crystals that are sufficiently large for neutron diffraction studies. Thus, improvement of crystal growth to obtain large-volume crystals for neutron diffraction is a current area of interest in structural biology.

Human fibroblast growth factor 1 (FGF-1) is an important pro-angiogenic factor for human therapeutic application and its X-ray structure has been solved to 1.10 Å resolution (Bernett *et al.*, 2004; Fig. 1). However, the characteristic $C222_1$ orthorhombic space group yields crystals with thin plate-type morphology with crystal volumes typically of <1.0 mm^3 and this effectively prevents neutron diffraction studies. The thin physical dimension of these crystals corresponds to the *b* cell edge (Honjo *et al.*, 2008). The X-ray data indicate the presence of a crystallographic twofold axis of symmetry (involving the x, $-y$, $-z$ operator) adjacent to residue Glu81. This intermolecular crystal contact appears to be tenuous in that it is mediated exclusively by solvent and there are no direct intermolecular contacts (Fig. 2*a*). Furthermore, the local residues involved in this interface include Glu, Lys and Gln residues with high side-chain entropy values, which negatively correlate with crystallization (Longenecker *et al.*, 2001; Mateja *et al.*, 2002; Derewenda, 2004; Cooper *et al.*, 2007).

A previous study of Ala, Leu, Ser and Thr mutations at position 81 in FGF-1 showed that crystal growth along the *b* cell edge was improved with E81S and E81T mutants but not with E81A or E81L

Table 1
Crystal, data-collection and refinement statistics for FGF-1 crystal-packing mutants.

Values in parentheses are for the highest resolution shell.

	Wild type†	E81A/K101A	E81A/E82N/K101A	E81S/K101A	E81S/E82N/K101A
Space group	$C222_1$	$C222_1$	$C222_1$	$C222_1$	$C222_1$
Unit-cell parameters (Å)					
a	74.1	73.3	74.7	77.9	77.9
b	96.8	97.9	95.8	92.4	93.2
c	109.0	108.4	108.2	107.5	107.1
Maximum resolution (Å)	1.65	1.80 (1.91–1.80)	1.85 (1.89–1.85)	2.15 (2.20–2.15)	2.10 (2.15–2.10)
Mosaicity (°)		0.47	0.41	1.05	0.84
Molecules per ASU	2	2	2	2	2
Matthews coefficient (Å^3 Da^{-1})	2.96	2.92	2.91	2.91	2.92
Total reflections		274769	204098	89819	121150
Unique reflections		34332	30785	21461	22850
Redundancy		3.5	4.0	4.2	2.6
Completeness (%)		93.9 (58.4)	91.7 (54.8)	99.8 (99.9)	98.9 (88.4)
$I/\sigma(I)$		12.6 (2.9)	16.2 (5.7)	6.8 (3.1)	12.5 (2.9)
R_{merge} (%)		7.6 (34.6)	5.3 (19.8)	8.3 (38.0)	6.4 (25.2)
R_{cryst} (%)		19.0	19.0	18.1	21.0
R_{free} (%)		21.5	22.6	22.5	24.9
R.m.s.d. bond length (Å)		0.014	0.016	0.010	0.011
R.m.s.d. bond angle (°)		1.67	1.73	1.46	1.50
Ramachandran plot‡					
Favored (%)		97.5	96.8	97.1	96.8
Allowed (%)		2.5	3.2	2.9	3.2
Outliers (%)		0.0	0.0	0.0	0.0
PDB code		3cqa	3crg	3crh	3cri

† Kim *et al.* (2002). ‡ Davis *et al.* (2007).

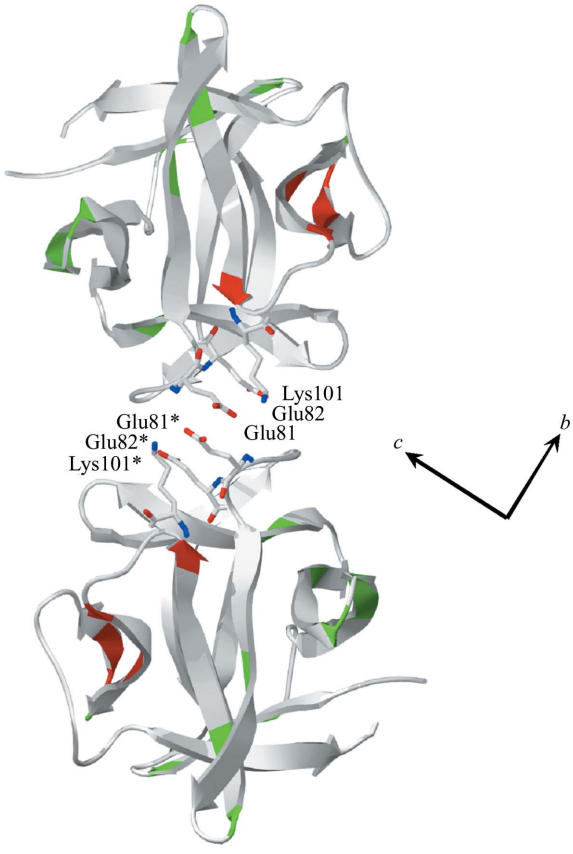

Figure 1
A ribbon diagram of wild-type FGF-1 (PDB code 1jqz, molecule *A*) indicating the twofold crystal contact (involving the $x, -y, -z$ symmetry operator) adjacent to position Glu81. Also shown are the side chains of Glu82 and Lys101 (the positions subjected to mutation to improve this crystal contact); symmetry-related positions are indicated with asterisks. Green positions indicate the molecular interface with the FGF receptor and red positions indicate the molecular interface with heparin (Stauber *et al.*, 2000; Schlessinger *et al.*, 2000). The orientation of the cell edges are indicated (the view is down the *a* cell edge).

(despite a reduction in side-chain entropy for all mutants; Honjo *et al.*, 2008). These results also demonstrated the introduction of a novel direct intermolecular contact between Ser81 and (symmetry-related) Lys101 across the crystallographic twofold. In the present study, we have attempted additional engineering of this crystal contact to eliminate high-entropy side chains and to replace solvent-mediated intermolecular contacts with direct intermolecular contacts. The mutant studies were performed in various combinations and suggest that mutations to increase direct molecular contacts between the packing interface are more successful than mutations to reduce side-chain entropy in increasing crystal growth along the *b* cell edge.

2. Materials and methods

2.1. Mutagenesis and expression

Throughout the text, the mutant nomenclature utilizes the single-letter amino-acid code, *e.g.* E81S refers to glutamate at position 81 substituted by serine. The mutant design involved various combinations of the side-chain entropy-reducing mutations E81A, E81S, E82N and K101A; these mutations also result in charge neutralization. All mutant FGF-1 proteins utilized a synthetic gene for the 140-amino-acid form of human FGF-1 (Gimenez-Gallego *et al.*, 1986; Linemeyer *et al.*, 1990; Ortega *et al.*, 1991; Blaber *et al.*, 1996) containing an additional amino-terminal six-His tag as previously described (Brych *et al.*, 2001). Complementary primers of 32–33 bases were commercially synthesized and the QuikChange site-directed mutagenesis protocol (Agilent Technologies, Santa Clara, California, USA) was used to introduce all mutations, which were subsequently confirmed by nucleic acid sequence analysis (Biomolecular Analysis Synthesis and Sequencing Laboratory, Florida State University). The mutant proteins were expressed in *Escherichia coli* BL21 (DE3) cells and purified to homogeneity using Ni–NTA and heparin Sepharose chromatography as previously described (Brych *et al.*, 2001). The purified proteins were dialyzed against 50 m*M* sodium phosphate buffer pH 7.5 containing 100 m*M* NaCl, 10 m*M* ammonium sulfate, 0.5 m*M* EDTA and 2 m*M* DTT for crystallographic studies.

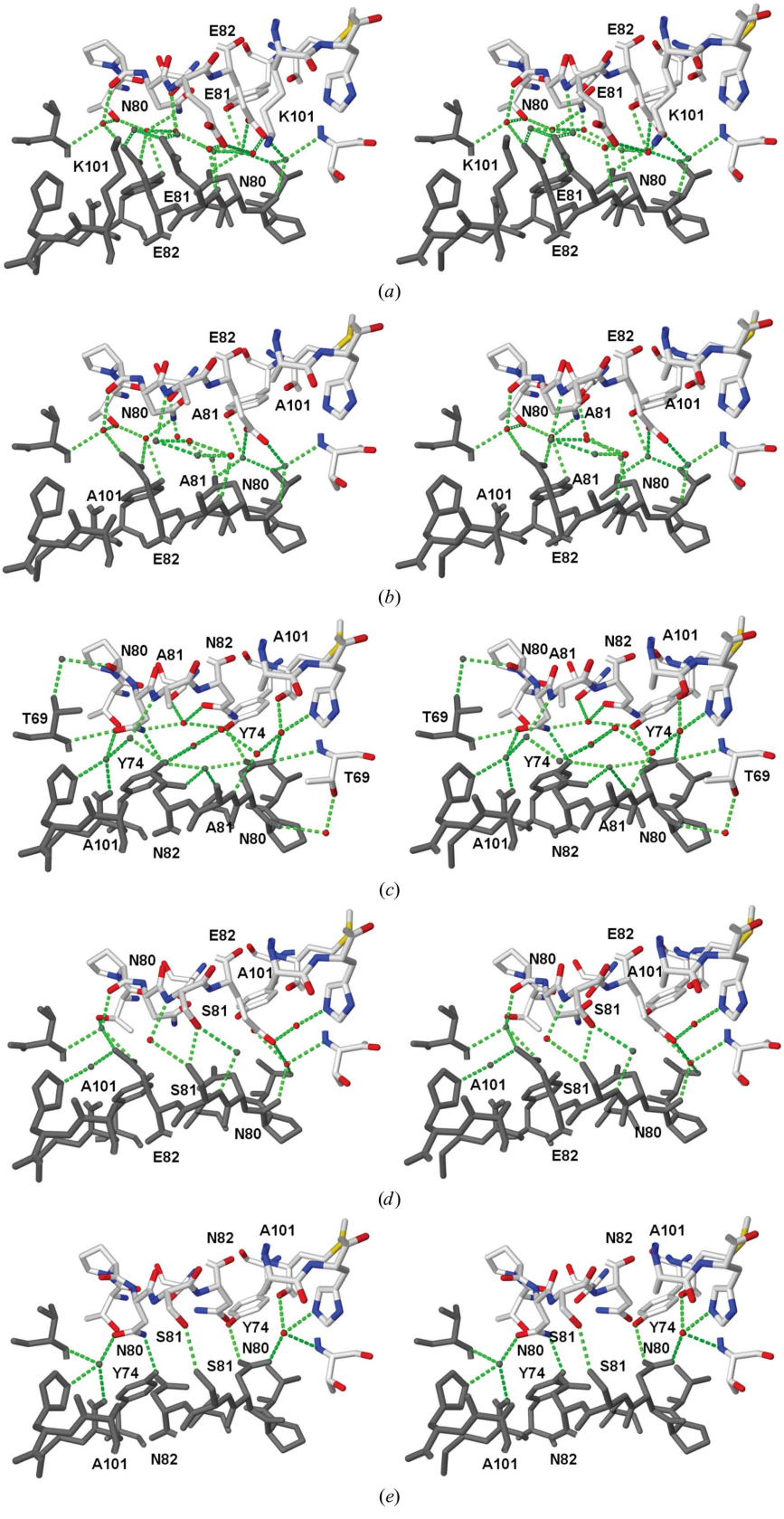

Figure 2
A relaxed stereo diagram detailing the crystal-packing interface along the *b* cell edge of the wild-type $C222_1$ orthorhombic space group and involving a twofold axis of crystallographic symmetry adjacent to position 81. (*a*) Wild-type FGF-1, (*b*) E81A/K101A mutant, (*c*) E81A/E82A/K101A mutant, (*d*) E81S/K101A mutant, (*e*) E81S/E82N/K101A mutant. Only the intermolecular hydrogen bonds are shown in each case.

2.2. Crystallization, data collection and refinement

The mutant proteins were concentrated to 4–16 mg ml^{-1} and crystals were grown using the hanging-drop vapor-diffusion method against 1 ml reservoirs containing sodium formate precipitant with or without 0.4 *M* ammonium sulfate. Crystallization trials were maintained at 298 K for one week. Crystals were flash-cryo-cooled in a stream of gaseous nitrogen at 100 K and diffraction data were collected in-house using a Rigaku RU-H2R rotating-anode X-ray source (Rigaku MSC, The Woodlands, Texas, USA) equipped with Osmic Blue confocal mirrors (MAR USA, Evanston, Illinois, USA) and a Rigaku R-AXIS IIc image-plate detector. The diffraction data were indexed, integrated and scaled using the *HKL*-2000 software (Otwinowski, 1993; Otwinowski & Minor, 1997). Molecular replacement utilized the structure of wild-type FGF-1 (PDB code 1jqz; Brych *et al.*, 2001) and the *Crystallography and NMR System* (*CNS*) software (Brünger *et al.*, 1998). 5% of the data were extracted for calculation of $R_{\rm free}$ (Brünger, 1992) and refinement was performed using the *CNS* software with simulated annealing and a maximum-likelihood target (Brünger *et al.*, 1998). Model building was performed using the program *O* (Jones *et al.*, 1991).

3. Results

Diffraction-quality crystals were obtained for the E81A/K101A, E81A/E82N/K101A, E81S/K101A and E81S/E82N/K101A mutants and proved to be isomorphous to the wild-type $C222_1$ space group in each case (Table 1). Of these mutants, the E81S/E82N/K101A mutant yielded consistently thicker dimensions corresponding to the *b* cell edge (Fig. 3), while the others were essentially indistinguishable from the wild-type crystal morphology. Multiple measurements of well formed single crystals indicated that the crystal volume increased from an average of 0.3 mm^3 (for the wild type) to 0.6 mm^3 (for the E81S/E82N/K101A mutant), with individual crystals of the E81S/E82N/K101A mutant achieving crystal volumes of up to ∼1.0 mm^3. Diffraction data sets with resolution limits of 1.80–2.15 Å were collected for this set of mutants with good data-collection and refinement statistics (Table 1). All mutant positions could be unambiguously modeled into the $2F_{\rm o} - F_{\rm c}$ OMIT map density and all structures were refined with acceptable stereochemistry and values of crystallographic residuals (Table 1). A brief description of the crystal contact details for each mutant form is provided below.

3.1. E81A/K101A

The unit-cell parameters of this mutant are essentially identical to those of the wild-type protein (Table 1). As for the wild-type protein, the twofold-symmetry contact in the region of residue 81 is mediated exclusively by solvent molecules (Fig. 2*b*). However, instead of four solvent molecules bridging this intermolecular crystal contact (with two on each side of the twofold axis), only three are observed (with one on each side of the twofold axis and a third centrally located solvent). The central solvent in this cluster has two alternative closely spaced positions and each has 50% occupancy.

3.2. E81A/E82N/K101A

The unit-cell parameters of this mutant are also essentially identical to those of the wild-type protein (Table 1); however, there are several side-chain conformational changes in the region of the crystal contact. The introduced Asn82 side chain adopts a *gauche*$^-$ ($\chi_1 \simeq +60^\circ$) rotamer orientation instead of the *gauche*$^+$ ($\chi_1 \simeq -60^\circ$) orientation observed for the wild-type Gln82 side chain (Fig. 2*c*). The adjacent Asn80 side chain similarly changes rotamer orientation from *gauche*$^-$ ($\chi_1 \simeq +60^\circ$) in the wild-type structure to *gauche*$^+$ ($\chi_1 \simeq -60^\circ$). In this orientation, the Asn80 side chain displaces a local solvent molecule and the Asn80 $O^{\delta1}$ group hydrogen bonds directly to the main-chain amide of the symmetry-related position Thr69. Furthermore, the repositioned Asn80 $N^{\delta2}$ group hydrogen bonds directly to the O^{η} group of the symmetry-related position Tyr74. The Thr69 side chain changes rotamer orientations, permitting the $O^{\gamma1}$ group to hydrogen bond *via* solvent to the main-chain carbonyl of the symmetry-related position Pro79. The solvent structure within the crystal-packing interface is similar to that of the E81A/K101A mutant, with the inclusion of two additional solvent molecules (on each side of the twofold axis), forming a more extensive hydrogen-bond network.

3.3. E81S/K101A

Although isomorphous to the wild-type protein, this mutant exhibits an ∼4 Å reduction in the *b* unit-cell parameter and a similar increase in the *a* unit-cell parameter (Table 1). The solvent structure at the twofold interface is similar to that observed in the E81A/K101A mutant; however, four solvent molecules within the interface have been excluded in response to the closer packing across the twofold (compare Fig. 2*d* with Fig. 2*b*). The distance between the symmetry-related Ser81 O^{γ} groups across the twofold axis is 2.51 Å, suggesting a strong hydrogen bond (see §4).

3.4. E81S/E82N/K101A

Similar to the E81S/K101A mutant, this mutant exhibits an ∼4 Å reduction in the *b* unit-cell parameter and a similar increase in the *a* unit-cell parameter (Table 1). The Asn80 and Asn82 side-chain rotamers are similar to those observed in the E81A/E82N/K101A structure (compare Fig. 2*e* with Fig. 2*c*) and the E81S side chain rotamer is essentially identical to that observed in the E81S/K101A mutant (compare Fig. 2*e* with Fig. 2*d*). The twofold intermolecular contact now involves a series of direct intermolecular contacts instead of the solvent-mediated interface present in the wild-type structure (compare Fig. 2*e* with Fig. 2*a*).

4. Discussion

In the present study, we have focused upon improving a specific twofold crystal contact (adjacent to position 81) in the isomorphous FGF-1 $C222_1$ crystal form, with the goal of increasing crystal growth along the thin *b* cell edge. The selected mutations were intended to probe the effects of decreasing the side-chain entropy, as well as charge neutralization, at the site of a crystallographic twofold molecular contact; however, the X-ray structures show that some mutations also change the interface from a solvent-mediated to a direct molecular contact.

The E81A/K101A mutant reduces the side-chain entropy associated with the Gln81 and Lys101 side chains at this crystal contact. Additionally, the E81A mutation eliminates the electrostatic charge–charge repulsion present in the wild-type intermolecular contact (Fig. 2*a*). Despite this reduction in side-chain entropy, essentially no improvement is observed in the *b* cell-edge thickness. The E81A/E82N/K101A mutant further reduces the side-chain entropy at this interface (by inclusion of the E82N mutation). Significant rearrangement of the rotamer orientations in the region of the twofold contact are observed; however, no improvement in the *b* cell-edge thickness is observed. The E81S/K101A mutant reduces the side-chain entropy and also introduces a direct intermolecular contact (involving Ser81 across the twofold). This intermolecular contact (2.51 Å) suggests a strong hydrogen bond; however, a purely twofold-symmetric relationship would require a donor–donor or acceptor–

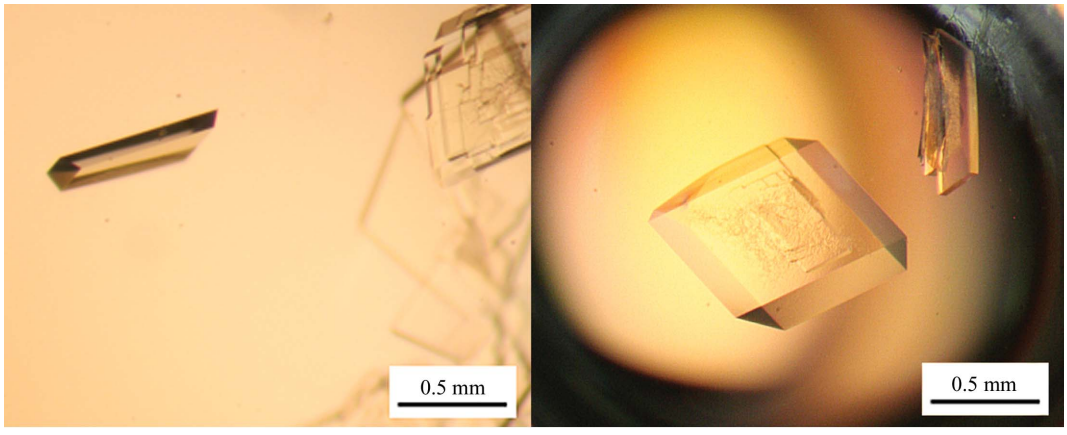

(*a*) (*b*)

Figure 3
Characteristic crystal morphology of wild-type FGF-1 (*a*l) and the E81S/E82N/K101A crystal contact mutant (*b*). The E81S/E82N/K101A mutant demonstrates an increase in direct intermolecular contacts and a corresponding improvement in the crystal thickness along the *b* cell edge.

acceptor interaction. Since the most likely interaction is a donor–acceptor interaction, pure twofold symmetry appears to be broken. Nonetheless, the wild-type $C222_1$ space group is correct and it is only on consideration of the hydrogen positions (which are invisible to X-ray diffraction at this resolution) that the symmetry is broken. Thus, for neutron diffraction studies a lower symmetry space group would be called for. The E81S/K101A/E82N mutant combines both a reduction in side-chain entropy and an increase in direct molecular contact across the crystal-packing interface. In fact, with this mutant the exclusively solvent-mediated interaction observed in the wild-type protein is replaced by an interface that is essentially composed of a series of direct molecular contacts. It is only with this mutant that an improvement in crystal growth along the *b* cell edge is observed. Despite this increase in crystal growth we did not observe any noticeable improvement in diffraction resolution limit, although additional studies may be needed to characterize the X-ray absorptive effects ariding from the volume increase. The backbone atoms of the E81S/K101A/E82N mutant overlay those of the wild-type FGF-1 protein with a root-mean-square deviation of 0.28 Å (essentially the error of the data set). Thus, while the *a* cell edge has increased slightly, the overall structure and other crystal contact sites are essentially unchanged.

The results suggest that solvent-mediated crystal contacts may be less favorable for crystal growth than direct contacts. Furthermore, focusing upon the introduction of direct crystal contacts may provide greater success than focusing on mutations designed to simply reduce side-chain entropy. Finally, hydrogen-bond interactions across a twofold contact, while seemingly incompatible with pure twofold symmetry, may not violate this apparent symmetry when utilizing moderate-resolution X-ray diffraction data in which discrete H atoms are not resolved.

We thank Dr T. Somasundaram of the X-ray Crystallography Facility, Kasha Laboratory, Institute of Molecular Biophysics for valuable suggestions and technical assistance. We also thank Ms Pushparani Dhanarajan of the Molecular Cloning Facility, Department of Biological Science for technical assistance. This work was supported by grant 0655133B from the American Heart Association.

References

Adachi, M. *et al.* (2009). *Proc. Natl Acad. Sci. USA*, **106**, 4641–4646.
Bernett, M. J., Somasundaram, T. & Blaber, M. (2004). *Proteins*, **57**, 626–634.
Blaber, M., DiSalvo, J. & Thomas, K. A. (1996). *Biochemistry*, **35**, 2086–2094.
Blakeley, M. P., Mitschler, A., Mazemann, I., Meilleur, F., Myles, D. A. & Podjarny, A. (2006). *Eur. Biophys. J.* **35**, 577–583.
Brünger, A. T. (1992). *Nature (London)*, **355**, 472–475.
Brünger, A. T., Adams, P. D., Clore, G. M., DeLano, W. L., Gros, P., Grosse-Kunstleve, R. W., Jiang, J.-S., Kuszewski, J., Nilges, M., Pannu, N. S., Read, R. J., Rice, L. M., Simonson, T. & Warren, G. L. (1998). *Acta Cryst.* D**54**, 905–921.
Brych, S. R., Blaber, S. I., Logan, T. M. & Blaber, M. (2001). *Protein Sci.* **10**, 2587–2599.
Cooper, D. R., Boczek, T., Grelewska, K., Pinkowska, M., Sikorska, M., Zawadzki, M. & Derewenda, Z. (2007). *Acta Cryst.* D**63**, 636–645.
Davis, I. W., Leaver-Fay, A., Chen, V. B., Block, J. N., Kapral, G. J., Wang, X., Murray, L. W., Arendall, W. B. III, Snoeyink, J., Richardson, J. S. & Richardson, D. C. (2007). *Nucleic Acids Res.* **35**, W375–W383.
Derewenda, Z. S. (2004). *Structure*, **12**, 529–535.
Gimenez-Gallego, G., Conn, G., Hatcher, V. B. & Thomas, K. A. (1986). *Biochem. Biophys. Res. Commun.* **128**, 611–617.
Honjo, E., Tamada, T., Adachi, M., Kuroki, R., Meher, A. & Blaber, M. (2008). *J. Synchrotron Rad.* **15**, 285–287.
Jones, T. A., Zou, J.-Y., Cowan, S. W. & Kjeldgaard, M. (1991). *Acta Cryst.* A**47**, 110–119.
Kim, J., Blaber, S. I. & Blaber, M. (2002). *Protein Sci.* **11**, 459–466.
Linemeyer, D. L., Menke, J. G., Kelly, L. J., Disalvo, J., Soderman, D., Schaeffer, M.-T., Ortega, S., Gimenez-Gallego, G. & Thomas, K. A. (1990). *Growth Factors*, **3**, 287–298.
Longenecker, K. L., Garrard, S. M., Sheffield, P. J. & Derewenda, Z. S. (2001). *Acta Cryst.* D**57**, 679–688.
Mateja, A., Devedjiev, Y., Krowarsch, D., Longenecker, K., Dauter, Z., Otlewski, J. & Derewenda, Z. S. (2002). *Acta Cryst.* D**58**, 1983–1991.
Niimura, N. & Bau, R. (2008). *Acta Cryst.* A**64**, 12–22.
Ortega, S., Schaeffer, M.-T., Soderman, D., DiSalvo, J., Linemeyer, D. L., Gimenez-Gallego, G. & Thomas, K. A. (1991). *J. Biol. Chem.* **266**, 5842–5846.
Otwinowski, Z. (1993). *Proceedings of the CCP4 Study Weekend. Data Collection and Processing*, edited by L. Sawyer, N. Isaacs & S. Bailey, pp. 56–62. Warrington: Daresbury Laboratory.
Otwinowski, Z. & Minor, W. (1997). *Methods Enzymol.* **276**, 307–326.
Schlessinger, J., Plotnikov, A. N., Ibrahimi, O. A., Eliseenkova, A. V., Yeh, B. K., Yayon, A., Linhardt, R. J. & Mohammadi, M. (2000). *Mol. Cell. Biol.* **6**, 743–750.
Stauber, D. J., DiGabriele, A. D. & Hendrickson, W. A. (2000). *Proc. Natl Acad. Sci. USA*, **97**, 49–54.
Tuan, H.-F., Erskine, P., Langan, P., Cooper, J. & Coates, L. (2007). *Acta Cryst.* F**63**, 1080–1083.